Preprint typeset using LaTeX style emulateapj v. 2/19/04

BLAZARS AS ULTRA-HIGH-ENERGY COSMIC-RAY SOURCES: IMPLICATIONS FOR TEV GAMMA-RAY OBSERVATIONS

KOHTA MURASE[1], CHARLES D. DERMER[2], HAJIME TAKAMI[3], AND GIULIA MIGLIORI[4]

ABSTRACT

Spectral fitting of correlated multiwavelength data of BL Lac objects and Fanaroff-Riley I radio galaxies gives the mean comoving magnetic field strength B', the bulk outflow Doppler factor Γ, and the emission region size R' of the radiating plasma in the one-zone leptonic synchrotron self-Compton (SSC) model. From the Hillas condition, we show that only in rare cases can these sources accelerate protons to much above 10^{19} eV, so $\gtrsim 10^{20}$ eV ultra-high-energy cosmic rays are likely to be heavy ions if powered by this type of AGN. One of the signatures of hadronic production by blazars is intergalactic cascade emission initiated by ultra-high-energy cosmic rays, which can explain TeV spectra of some extreme, apparently non-variable blazars such as 1ES 0229+200. We study this kind of cascade signal from such blazars, taking into account effects of the structured extragalactic magnetic fields in clusters and filaments in which the blazars are embedded. We demonstrate the importance of cosmic-ray deflections on the gamma-ray flux, and show that large cosmic-ray luminosities are typically required to explain their spectra for the maximum cosmic-ray energy inferred by the one-zone SSC model for variable BL Lac objects and radio galaxies. The hadronic interpretation of the gamma-ray emission of TeV blazars require strong, $B' \sim 10-100$ G magnetic fields, where acceleration of protons to $\gtrsim 10^{20}$ eV is possible, rather than the lower magnetic fields found in the leptonic synchrotron/SSC modeling. While hadronic models could be confirmed by neutrino detection from luminous blazars, future TeV gamma-ray observations with the Cherenkov Telescope Array and the High Altitude Water Cherenkov detector array can also achieve this goal by detecting > 25 TeV photons from relatively low-redshift sources such as 1ES 0229+200, and $\gtrsim$ TeV photons from more distant sources.

Subject headings: galaxies: active — gamma rays: galaxies — cosmic rays

1. INTRODUCTION

Active galactic nuclei (AGN) with extended radio jets powered by super-massive black holes are among the most luminous objects in the low-redshift universe. Since 2004, when the present generation of imaging atomspheric Cherenkov telescopes began to operate, the number of blazars and radio galaxies detected at $\gtrsim 0.1$ TeV (very-high energy; VHE) energies has grown rapidly, and now is nearly fifty[5]. The *Fermi* Gamma-ray Space Telescope, now three years into its mission, is providing a compendium of new discoveries on gamma-ray emitting galaxies. In the high-confidence clean sample of active galactic nuclei associations in the First *Fermi* LAT AGN catalog (1LAC; Abdo et al. 2010a), more than 600 gamma-ray blazars, divided about equally into BL Lac objects and flat spectrum radio quasars (FSRQs), were reported. New classes of GeV gamma-ray galaxies, e.g., radio-loud narrow line Seyfert galaxies (Abdo et al. 2009a) and star-forming galaxies powered by supernovae (rather than black holes; Abdo et al. 2010b) are now firmly established. Though yet to be fully deciphered, the gamma-ray spectral energy distributions (SEDs) of radio galaxies, being misaligned by large ($\gtrsim 10^\circ$) angles to the jet axis and thought to be the parent population of blazars in geometrical unification scenarios (Urry & Padovani 1995), reveal the blazar jet geometry. At least 11 such sources are now detected with *Fermi* (Abdo et al. 2010c).

Radio-loud AGN detected at TeV energies consist mainly of high-synchrotron-peaked BL Lac objects, including the ultra-variable TeV blazars Mrk 421 (z=0.031; Fossati et al. 2008), Mrk 501 (z=0.033; Albert et al. 2007) and PKS 2155-304 (z=0.116; Aharonian et al. 2007a), and the apparently steady or weakly variable TeV blazars 1ES 0229+200 (Aharonian et al. 2007b) and 1ES 1101-232 (Aharonian et al. 2007c). Extragalactic VHE gamma-ray galaxies also now include several Fanaroff-Riley (FR) class I radio galaxies (Cen A, M87, NGC 1275; Abdo et al. 2010d; Abdo et al. 2009c; Abdo et al. 2009b, respectively), the head-tail radio galaxy IC 310 (Neronov et al. 2010 ; Aleksić et al. 2010), intermediate-synchrotron-peaked objects like 3C 66A (Abdo et al. 2011a) and BL Lac (Abdo et al. 2011b), and the GeV luminous, high-redshift FSRQs 3C 279 (z=0.538; Aleksić et al. 2011a), PKS 1510-089 (z=0.361; Wagner et al. 2010), and 4C +21.35 (PKS 1222+216, z=0.432; Aleksić et al. 2011b).

The gamma-ray data from weak-lined BL Lac objects and FR-I radio galaxies are generally well fit with the standard nonthermal electronic synchrotron self-Compton (SSC) relativistic jet model (e.g., Mastichiadis & Kirk 1997; Tavecchio et al. 1998; Kato et al. 2006), but the use of archival data for highly variable blazars gave large parameter uncertainties in the past. With the recent contemporaneous multi-wavelength data sets for many sources, accurate parameter estimation can be made, either from simple scaling results in the Thomson regime, or from detailed spectral calculations, which is especially needed for high, UV/X-ray synchrotron-peaked blazars with scattering in the extreme Klein-Nishina (KN) regime.

In Section 2, we assemble the derived parameter values ob-

[1] Department of Physics, Center for Cosmology and Astro-Particle Physics, The Ohio State University, Columbus, OH 43210, USA
[2] Space Science Division, Naval Research Laboratory, Washington, DC 20375, USA
[3] Max Planck Institute for Physics, Föhringer Ring 6, 80805 Munich, Germany
[4] Harvard-Smithsonian Center for Astrophysics, 60 Garden St., Cambridge, MA 02138, USA
[5] See tevcat.uchicago.edu/ and www.mpp.mpg.de/∼rwagner/sources/

tained in various analyses of typical BL Lac objects and FR-I radio galaxies. From these numbers, we obtain maximum energies of cosmic rays, and show that protons can be accelerated to $\gtrsim 10$ EeV energies only in a few radio galaxies and flares of BL Lac objects. Then we explore the associated hadronic signatures expected from TeV blazars in the case where jets of BL Lac objects and FR-I radio galaxies are accelerators of ultra-high-energy cosmic rays (UHECRs, with energies above the ankle of $\approx 10^{18.5}$ eV). We discuss observable signals produced at the source and calculate those generated outside the source from both gamma rays and UHECRs escaping from the jet accelerator and passing through the $\sim$ Mpc-scale regions of cosmic structure, magnetized clusters and filaments, and the larger ~ 100 Mpc-scale voids of intergalactic space. For some apparently non-variable TeV blazars, where the one-zone synchrotron/SSC model typically requires extreme parameters for fits, the cascade radiation can be a crucial component of the high-energy radiation spectrum, depending on the strength of the intergalactic magnetic field (IGMF) in voids, as has recently been proposed to explain the gamma-ray spectra of extreme blazars such as 1ES 0229+200 (Essey et al. 2010; Essey et al. 2011), and we focus on such cascade emissions in the VHE range in Section 3. Using numerical calculations, we also demonstrate the importance of structured extragalactic magnetic fields (EGMFs) in clusters and filaments for future gamma-ray detectability by the Cherenkov Telescope Array (CTA) and the High Altitude Water Cherenkov detectors (HAWC). Implications of the study and a summary are given in Section 4. Throughout this work, the cosmological parameters are taken as $H_0 = 71$ km s^{-1} Mpc^{-1}, $\Omega_m = 0.3$, and $\Omega_\Lambda = 0.7$.

2. VHE BLAZARS AND UHECRS

Of the wide variety of source classes that could potentially accelerate UHECRs, including, for example, GRBs (Waxman 1995; Vietri 1995; Murase et al. 2008a), fast rotating magnetars (Arons 2003), structure formation shocks in galaxy clusters (Norman et al. 1995; Kang et al. 1996; Inoue et al. 2007), and quasar remnants (Boldt & Ghosh 1999; Levinson 2000), AGN with jets seem privileged in that the most pronounced excess in arrival directions of UHECRs is positionally centered in the vicinity of the FR-I radio galaxy Centaurus A (Abraham et al. 2008; Abraham et al. 2009)[6]. FR-I radio galaxies, including their aligned BL Lac counterparts, are found within the ≈ 100 Mpc Greisen-Zatsepin-Kuzmin radius and radiate a volume- and time-averaged emissivity of $\approx 10^{45}$–10^{46} erg Mpc^{-3} yr^{-1} in nonthermal γ-rays (Dermer & Razzaque 2010). If comparable power goes into the acceleration of UHECRs, then BL Lac objects and FR-I radio galaxies have more than sufficient emissivity to power the $\gtrsim 10$ EeV UHECRs, which require $\sim 10^{44}$ erg Mpc^{-3} yr^{-1} (e.g., Waxman & Bahcall 1999; Berezinsky et al. 2006; Murase & Takami 2009).

2.1. *Two-Component Spectra of Blazars and Radio Galaxies*

When plotted as $\log(\nu F_\nu)$ vs. $\log(\nu)$, the typical two-humped SED of blazars and radio galaxies is characterized by peak synchrotron νF_ν flux at peak synchrotron photon energy ε_s, and peak inverse-Compton (IC) νF_ν flux at peak IC energy ε_C. The blazar spectrum is, in general, highly variable, and rises and decays with variability time $t_{\rm var}$, which can be taken as equal to the shortest significant factor-of-two change in flux in any waveband, assuming co-spatiality of the highly variable radiations as indicated by correlated variability. The synchrotron (IC) luminosities at peak energy are $L_\gamma^{s(C)} \approx 4\pi d_L^2(\varepsilon_{s(C)}F_\varepsilon^{s(C)})$ and the Compton dominance parameter is defined as $A_C \equiv L_\gamma^C/L_\gamma^s \approx (\varepsilon_C F_\varepsilon^C)/(\varepsilon_s F_\varepsilon^s)$.

In a relativistic spherical blob formalism, the Doppler factor is (Ghisellini et al. 1996)

$$\delta \simeq \frac{3^{1/2}(L_\gamma^s)^{1/4}(\varepsilon_C/m_e c^2)^{1/2}}{2^{3/4}c^{3/4}t_{\rm var}^{1/2}A_C^{1/4}B_{\rm Q}^{1/2}(\varepsilon_s/m_e c^2)}\,. \tag{1}$$

and the comoving magnetic field is

$$B' \simeq (1+z)\frac{2^{11/4}c^{3/4}t_{\rm var}^{1/2}A_C^{1/4}B_{\rm Q}^{1/2}(\varepsilon_s/m_e c^2)^3}{3^{3/2}(L_\gamma^s)^{1/4}(\varepsilon_C/m_e c^2)^{3/2}}$$
$$\simeq (1+z)\frac{4B_{\rm Q}(\varepsilon_s/m_e c^2)}{3\delta(\varepsilon_C/\varepsilon_s)}\,, \tag{2}$$

provided the Compton scattering takes place in the Thomson regime, which applies when $\delta \gg \delta_T = 2\sqrt{3}\sqrt{\varepsilon_s\varepsilon_c}(1+z)$. Here the critical magnetic field is $B_{\rm Q} \equiv m_e^2c^3/e\hbar \simeq 4.4\times 10^{13}$ G. The above equations are derived by using the relations $B'^2/8\pi \approx L_\gamma^s/(4\pi R'^2\delta^4 cA_C)$, $\varepsilon_s \approx \delta(B'/B_{\rm Q})\gamma_b'^2/(1+z)$, and $\varepsilon_c \approx (4/3)\gamma_b'^2\varepsilon_s$. Furthermore, the typical fluid-frame Lorentz factor of electrons radiating near the peak synchrotron and SSC frequencies is $\gamma_b' \approx (\sqrt{3}/2)\sqrt{\varepsilon_c/\varepsilon_s}$ in the Thomson limit. For high-peaked BL Lac objects, the Compton scattering often occurs in the Klein-Nishina regime, where more detailed modeling is required. Nevertheless, equations (1) and (2) demonstrate that source parameters such as δ and B' can be determined from the two humped SED.

Table 1 gives measured and inferred properties for blazars with good multiwavelength coverage that are well described by a synchrotron/SSC model, where derived values of magnetic fields and Doppler and Lorentz factors based on synchrotron self-Compton modeling are taken from the literature. For blazars, we assume that $\Gamma \approx \delta$, whereas values of the angle of the jetted emission with respect to the observer inferred from observations are considered for radio galaxies.

2.2. *Implications for UHECR Acceleration*

The Hillas condition (Hillas 1984) limits the maximum accelerated energy of ions with charge Z to

$$E_A^{\rm max} \approx ZeB'\Gamma R' \simeq Ze\frac{4(L_\gamma^s)^{1/4}t_{\rm var}^{1/2}B_{\rm Q}^{1/2}\varepsilon_s}{3c^{3/4}A_C^{1/4}\varepsilon_C^{1/2}}, \tag{3}$$

in order that the particle Larmor radius is smaller than the characteristic size scale $R' \lesssim ct_{\rm var}' = c\delta t_{\rm var}/(1+z)$. The inequality is replaced by an equality in our estimates. The final relation in equation (3) is obtained from the Thomson-limit relations given above when $\delta \approx \Gamma$.

Table 2 gives results of synchrotron/SSC model fits for these sources found in dedicated modeling papers, along with comoving magnetic fields and Doppler factors obtained from equation (2) and (3) (only when $\delta > \delta_T$). The proton maximum energy is estimated using equation (3) from parameters given in Table 1, noting that other losses and details of the acceleration process could limit the maximum particle energy

[6] See Takami & Sato 2009 for discussions on issues of UHECR anisotropy for protons, and Lemoine & Waxman 2009; Abreu et al. 2011 for heavy nuclei. Note also the potential contribution from the background Centaurus supercluster pointed out by Ghisellini et al. (2008).

TABLE 1
MEASURED AND INFERRED PROPERTIES OF VHE BLAZARS AND RADIO GALAXIES

ID	Source	z	Epoch	$t_{\rm var}$ [s]	$\delta^{(a)}$	$\Gamma^{(a)}/\theta_{\rm obs}^{(a,b)}$ /[deg]	$\gamma_b'^{(a)}$	$\varepsilon_s^{(a)}$ [$m_e c^2$]	$\nu_s F_\nu^{s(a)}[10^{-10}]$ [erg cm^{-2} s^{-1}]	$R'^{(a)}[10^{15}]$ [cm]	$B'^{(a)}$ [G]	$\varepsilon_C^{(a)}$ [$m_e c^2$]	$\nu_C F_\nu^{C(a)}[10^{-10}]$ [erg cm^{-2} s^{-1}]	Ref.
1	CenA(core)	0.00183	2009	$\leq 1.0\times10^5$	1.0-3.9	2.0-7.0/15-30	$(0.8-400)\times10^3$	$(0.8-4000)\times10^{-7}$	0.09-4.5	3.0	0.02-6.2	0.17-(8.3×10^5)	0.025-8.5	1
2	M87	0.00436	2009	1.7×10^5	3.9	2.3/10	4×10^3	1.6×10^{-7}	0.06	14.0	0.055	18.6	0.068	2
3	NGC1275	0.0179	Oct. 2010[d]	8.6×10^4	2.3	1.8/25	960	2.4×10^{-3}	0.9	2×10^3	0.05	2.9×10^3	0.3	3
4	NGC6251	0.024	–	–	2.4	2.4/25	2×10^4	6.5×10^{-7}	0.012	120	0.037	7.3	0.047	4
5	Mrk421	0.03	19 March 2001	1.0×10^3	80	80	9.3×10^4	0.005	7.4	3.0	0.048	8.1×10^4	7.0	5
6	Mrk501(h.[c],1997)	0.0337	16 April 1997	7×10^3	14-20	14-20	$(7-300)\times10^4$	0.3-0.5	8.0-8.5	1.0–4.3	0.2-0.8	$(1.4-2.6)\times10^6$	2.9-3.4	6,7,8
7	Mrk501 (l.[c],1997)	0.0337	7 April 1997	–	15	15	6×10^5	0.002	0.63	5.0	0.8	4.4×10^5	0.4	6
8	Mrk501 (l.[c],2007)	0.0337	2007	–	25	25	1×10^5	0.002	0.63	1.0	0.31	4.4×10^5	0.4	9
9	Mrk501 (l.[c],2009)	0.0337	2009	3.5×10^5	12-20	12-20	$(6-90)\times10^4$	0.002	0.55-0.63	1.0–130	0.015-0.31	$(1.3-4.4)\times10^5$	0.3-0.4	7,10,11
10	1ES1959+650(h.[c])	0.047	Sept2001-May2002	$(2.2-7.2)\times10^4$	18-20	14-20	$4-5\times10^4$	$(0.07-8)\times10^{-3}$	1.0-3	5.8-9	0.04-0.9	$8\times10^{5-6}$	0.2-2	12,13
11	1ES1959+650(l.[c])	0.047	23-25 May2006	8.64×10^4	18	18	5.7×10^4	0.003	2.6	7.3	0.25-0.4	1.2×10^5	0.22	14,15
12	PKS2200+420/BL Lac	0.069	–	–	15	15	900.0	5.3×10^{-7}	0.76	2.0	1.4	1.6	0.4	14
13	PKS2005-489	0.071	–	–	22	22	1.3×10^4	4.7×10^{-5}	1.5	8.0	0.7	3.6×10^3	0.07	14
14	WComae	0.102	7-8 June 2008	5400	20-25	20-25	$(1.5-20)\times10^4$	8.0×10^{-5}	0.4	3.0	0.3-0.24	8.1×10^3	0.15	14,16
15	PKS2155-304	0.116	28-30 July 2006	300	110	110	4.3×10^4	4×10^{-4}	2.13	0.86	0.1	9.7×10^5	20.0	5

[a]: parameter value from the SED modeling in literature (see references); [b]: for blazar sources $\delta \approx \Gamma$ and $\theta_j \approx 1/\Gamma$; [c]: high (h.) and low (l.) state; References: 1- Abdo et al.(2010d) (see Figure 5 and Table 2 in the paper for the different models), 2- Abdo et al. (2009c), 3- Abdo et al. (2009b), 4- Migliori et al. (2011, accepted), 5- Finke et al. (2008), 6- Pian et al. (1998), 7- Acciari et al. (2011), 8- Katarzynski et al. (2005), 9- Albert et al. (2007), 10- Anderhub et al. (2009), 11- Abdo et al. (2011c), 12- Tagliaferri et al. (2003), 13- Krawczynski et al. (2004), 14- Tavecchio et al. (2010), 15- Tagliaferri et al. (2008), 16- Acciari et al. (2009).

further. For the cases considered in Table 1, it is barely possible to accelerate protons up to $\sim 10^{20}$ eV, whereas Fe nuclei could easily each reach $\gtrsim 10^{20}$ eV provided that they can survive photodisintegration. Even with the allowed spread in parameter values, this conclusion seems robust.

A similar conclusion is also reached when considering luminosity requirements for BL Lac objects and FR-I radio galaxies (Dermer & Razzaque 2010; Ghisellini et al. 2010). In the latter paper, physical parameters were obtained via spectral modeling using their one-zone leptonic model of all blazars with known redshift detected by the *Fermi* satellite during its first 3-month survey. The inferred magnetic luminosity of BL Lac objects is typically $L_B \sim 10^{46}\delta_1^2$ erg s^{-1} and almost all of them satisfy $L_B \lesssim 10^{47.5}\delta_1^2$ erg s^{-1}, where $\delta_1 = \delta/10$. On the other hand, the required magnetic luminosity for UHECR acceleration to $10^{20}E_{A,20}$ eV is $L_B \approx 10^{47.5}\Gamma_1^2 E_{A,20}^2 Z^{-2}$ erg s^{-1} where $\Gamma_1 = \Gamma/10$. Hence, it also suggests difficulties in acceleration of $\gtrsim 10^{20.5}$ eV protons in typical BL Lac objects, though the simple SSC model may not be applied to lower-peaked BL Lac objects and it is not so easy to have well-defined values of B' and δ.

If BL Lac objects and FR-I radio galaxies, as has often been considered (e.g., Tinyakov & Tkachev 2001; Berezinsky et al. 2002; Dermer et al. 2009), accelerate the UHECRs, then an UHE proton origin of the highest-energy cosmic rays is disfavored from spectral modeling if the standard synchrotron/SSC model is correct. Heavier nuclei can, however, be accelerated up to ultra-high energies. The composition of UHECRs is an open question, with both proton and heavy-ion dominated compositions having been claimed to be compatible with HiRes (Abbasi et al. 2010) and the Pierre Auger Observatory (PAO) (Abraham et al. 2010) data, respectively. As seen here, the standard model for gamma-ray emission from BL Lac objects and FR-I radio galaxies suggests a transition from proton to heavy-ion dominated composition at $\sim (10^{18}-10^{19})$ eV.

We have assumed that the gamma-ray component of typical TeV blazars and radio galaxies is dominated by the electronic Compton-scattering component in order that synchrotron theory can be used to derive the various parameters. Thus the hadronic gamma-ray flux must be considerably smaller for a consistent interpretation. Sufficiently high-energy protons and nuclei interact with synchrotron photons in the jet via the photomeson process, with photopion production efficiency $f_{p\gamma}$ for cosmic-ray protons estimated to be (e.g., Murase & Beacom 2010)

$$f_{p\gamma} \simeq 2.3\times10^{-4}\left(\frac{2.5}{1+\alpha}\right)L^s_{\gamma,46}t^{-1}_{\rm var,4}\delta_1^{-4}\left(\frac{1\ {\rm keV}}{\varepsilon_s}\right)\left(\frac{E_p}{E_p^b}\right)^{\alpha-1}, \quad (4)$$

where $E_p^b \simeq 1.6\times10^{16}$ eV $(\varepsilon_s/1\ {\rm keV})^{-1}\delta_1^2(1+z)^{-2}$ is the typical energy of a proton that interacts with a photon with ε_s. Also, α is the photon index at energies below or above ε_s. For $\alpha \approx 1.5$, which is typical of blazars at $E_p > E_p^b$, the photomeson production efficiency at $\sim 10^{19}$ eV becomes of order $f_{p\gamma} \sim 6\times10^{-3}$, which suggests that the photomeson process is inefficient for this kind of blazar (though it could be more efficient for low-peaked BL Lac objects and FSRQs). The efficiency can also be higher if Γ is lower, provided that Γ is consistent with synchrotron/SSC model fits and minimum Lorentz factor estimates inferred from, e.g., $\gamma\gamma$ opacity arguments.

Using the typical neutrino luminosity $L_\nu \sim (3/8)f_{p\gamma}L_{\rm CR}$ from such a high-peaked BL Lac object, one finds that the neutrino flux from an individual source is typically too low to be detected with IceCube. One can also see that the cumulative background flux from high-peaked BL Lac objects is low. The UHECR energy input in the local universe is $\sim 5\times10^{43}$ erg Mpc^{-3} yr^{-1} at 10^{19} eV (Murase & Takami 2009), so that assuming that such BL Lac objects and FR-I galaxies are the main UHECR sources, the expected cumulative muon neutrino background flux is estimated to be

$$E_\nu^2\Phi_\nu \sim 10^{-10}\ {\rm GeV\ cm^{-2}\ s^{-1}\ sr^{-1}}\left(\frac{f_{p\gamma}(20E_\nu)}{10^{-2}}\right)E^{2-p}_{\nu,17.7}f_z, \quad (5)$$

where p is the cosmic-ray spectral index and f_z is a prefactor coming from the redshift evolution of the sources. Low photomeson production efficiencies also follow if the UHECRs are heavy nuclei, whose losses are dominated by photodisintegration (see below). More luminous blazars, including low-peaked BL Lac objects, may however lead to higher photomeson production efficiencies, so that the cumulative neutrino background could be dominated by this class of AGN (Mücke et al. 2003).

Our evaluation is based on the standard synchrotron/SSC blazar model for BL Lac objects. Alternately, one could abandon the standard synchrotron/SSC blazar model and consider a highly magnetized, $\sim 10-100$ G jet model, which is needed in hadronic blazar models to accelerate protons to $\gtrsim 10^{20}$ eV (Aharonian 2000). Correspondingly, the minimum magnetic luminosity is estimated to be $L_B \approx 10^{47.5}$ erg s^{-1} $\Gamma_1^2 E_{p,20}^2$, which is larger than the typical synchrotron luminosity of BL Lac objects, $L_\gamma^s \sim 10^{46}$ erg s^{-1}. In hadronic models, gamma-ray emission is attributed to proton synchrotron radiation and/or proton-induced cascade emission, which requires that the cosmic-ray luminosity $L_{\rm CR} > L_\gamma^C = A_C L_\gamma^s$. In the proton synchrotron blazar model (Aharonian 2000; Mücke & Protheroe 2001; Mücke et al. 2003), proton synchrotron radiation is emitted up to energies $\varepsilon_s^{\rm max} \approx 4\Gamma_1$ TeV (in the limit that the maximum energy is determined by the synchrotron cooling) in efficient Fermi acceleration scenarios. The photomeson production efficiency for protons is strongly dependent on δ, but the condition $L_B \gg L_\gamma^s$ suggests that the synchrotron energy-loss is dominant at ultra-high energies where the proton synchrotron radiation is typically prominent at $\sim$ TeV energies (though the photohadronic cascade component may become relevant at lower energies). The strong magnetic field also suppresses electronic SSC emission because fewer electrons are needed to generate the same synchrotron flux.

2.3. *Survival of Nuclei in the Source*

If we accept the standard synchrotron/SSC model for TeV blazars, then protons cannot reach $\sim 10^{20}$ eV. For BL Lac objects and FR-I galaxies to be the sources of UHECRs, therefore, UHECRs would primarily be heavier nuclei. In such a scenario, one has to examine whether ions can survive photodisintegration losses (cf. Murase et al. 2008a; Wang et al. 2008; Pe'er et al. 2009). The photodisintegration opacity is estimated similarly to the photomeson production efficiency, and we find

$$\tau_{A\gamma}(E_A) \simeq 0.16\left(\frac{2.5}{1+\alpha}\right)L^s_{\gamma,46}t^{-1}_{\rm var,4}\delta_1^{-4}\left(\frac{\varepsilon_s}{1\ {\rm keV}}\right)^{-1}\left(\frac{E_A}{E_A^b}\right)^{\alpha-1}, \quad (6)$$

TABLE 2
INFERRED PROPERTIES OF VHE BLAZARS AND RADIO GALAXIES

ID	Source	d_L [Mpc]	$L^s_\gamma[10^{45}]$ [erg cm^{-2} s^{-1}]	$L^C_\gamma[10^{45}]$ [erg cm^{-2} s^{-1}]	A_C	$\gamma'^{(e)}_b$	$\delta^{(b)}_T$	$\delta^{(c)}$	$R'^{(d)}[10^{15}]$ [cm]	$B'^{(a)}$ [G]	$E^{\max(f)}_A/Z[10^{19}]$ [eV]
1	CenA(core)	3.7	$(0.15-7.3)\times10^{-4}$	$(0.04-14)\times10^{-4}$	0.3-1.9	890-2.1×10^4	9.9-(6×10^{-4})	0.12-3.7	3.0-12	0.02-9.1	0.004-3.3
2	M87	16.7	2.0×10^{-4}	2.3×10^{-4}	1.1	9.3×10^3	0.006	2.7	20	0.021	0.040
3	NGC1275	75.3	0.06	0.02	0.35	960	0.005	–	–	–	4.6
4	NGC6251	104	2×10^{-3}	6.6×10^{-3}	3.3	2.9×10^3	0.007	–	–	–	0.27
5	Mrk421	130.0	1.5	1.4	0.95	3.4×10^3	74	–	–	–	0.29
6	Mrk501 (h.$^{(g)}$,1997)	146.0	2.0-2.2	0.7-0.9	0.36-0.41	$(1.4\text{-}2.5)\times10^3$	$(3.0\text{-}3.5)\times10^3$	–	–	–	0.17-1.5
7	Mrk501 (l.$^{(g)}$,1997)	146.0	0.2-0.4	0.1-0.2	0.44-0.63	$(0.08\text{-}1.3)\times10^4$	100-1700	–	–	–	0.28-1.5
8	Mrk501 (l.$^{(g)}$,2007)	146.0	0.2	0.1	0.63	1.3×10^4	100	–	–	–	0.2
9	Mrk501 (l.$^{(g)}$,2009)	146.0	0.1-0.2	0.08-0.1	0.55-0.63	$(0.7-1.3)\times10^4$	58-100	–	–	–	0.12-0.6
10	1ES1959+650(h.$^{(g)}$)	206	0.5-1.5	0.1-1.1	0.2-0.8	$(2.7-9.5)\times10^4$	27-910	–	–	–	0.12-2.9
11	1ES1959+650(l.$^{(g)}$)	206	1.3	0.1	0.08	6600	66	–	–	–	1.3
12	PKS2200+420/BL Lac	307.0	0.8	0.45	0.53	2.8×10^3	0.006	–	–	–	1.1
13	PKS2005-489	316.0	1.8	0.07	0.04	7.6×10^3	1.5	–	–	–	3.1
14	WComae	464.0	1.0	0.38	0.38	8.7×10^3	3.1	7.2	3.0-3.7	2.1-2.6	0.37-0.57
15	PKS2155-304	533.0	7.2	68	9.4	1.3×10^4	24	–	–	–	0.23

$^{(a)}$: obtained from equation (2); $^{(b)}$: $\delta_T = 2\sqrt{3}\sqrt{\varepsilon_C\varepsilon_s}(1+z)$; $^{(c)}$: obtained from equation (1); $^{(d)}$: calculated assuming $R' \lesssim ct'_{\rm var} = c\delta t_{\rm var}/(1+z)$; $^{(e)}$: $\gamma'_b \approx \sqrt{3}/2\sqrt{\varepsilon_C/\varepsilon_s}$; $^{(f)}$: obtained from equation (3) using B', Γ, and R' reported in Table 1; $^{(g)}$: high (h.) and low (l.) state.

where $E^b_A \simeq 4.8\times10^{16}$ eV $(A/56)^{0.79}(\varepsilon_s/1\ {\rm keV})^{-1}\delta_1^2(1+z)^{-2}$ is the energy of a nucleus that typically interacts with a photon with ε_s. Hence, $\sim 10^{20.5}$ eV irons are more or less disintegrated unless $\delta \gtrsim 17(A/56)^{-0.158}(L^s_{\gamma,46})^{1/5}t_{\rm var,4}^{-1/5}(\varepsilon_s/1\ {\rm keV})^{-0.1}$ (for $\alpha\sim1.5$), but significant photodisintegration loss is easily avoided for reasonably large bulk outflow Doppler factors.

Recalling from equation (4) that the photomeson production efficiency has the same dependence on δ, we can conclude that when heavy nuclei survive photodisintegration, the photomeson production efficiency is so low that the corresponding neutrino and gamma-ray fluxes are not easily detected (Murase & Beacom 2010).

3. EXTREME TEV BLAZARS AND INTERGALACTIC CASCADES

TeV observations constrain bulk outflow Doppler factors δ from the $\gamma\gamma$ opacity argument, implying $\delta \gtrsim 60$ for PKS 2155-304 (Begelman et al. 2008) for the major July/August 2006 TeV flares (Aharonian et al. 2007a), and implying $\delta \gtrsim 100$ to be furthermore consistent with synchrotron/SSC model fitting for different models of the extragalactic background light (EBL; Finke et al. 2008). Another important fact is that VHE photons can interact with the cosmic photon backgrounds. VHE gamma rays produce electron-positron pairs via $\gamma\gamma$ pair creation, and the resulting high-energy pairs make high-energy photons via IC scattering. Hence, the cascaded gamma rays, which are often called pair echoes (e.g., Plaga 1995; Murase et al. 2008b) and/or pair haloes (e.g., Aharonian et al. 1994; Neronov & Semikoz 2007), are expected at GeV-TeV energies.

Many gamma-ray blazars show variability, and often display spectacular flares. Some of them are highly variable, as seen in multi-TeV flaring episodes from PKS 2155-304 (Aharonian et al. 2007a; Aharonian et al. 2009). But such rapidly varying gamma-ray emission should be produced near the source because of effects of the IGMF. Based on the lower limits of $B_{\rm IG}\lambda_{\rm coh}^{1/2} \gtrsim 10^{-18}-10^{-17}$ G Mpc$^{1/2}$ obtained for 1ES 0229+200 (Dolag et al. 2011; Dermer et al. 2011; Takahashi et al. 2011), the IGMF will introduce a significant time delay in the cascade radiation, which is incompatible with rapidly varying emissions. (The term $\lambda_{\rm coh}$ is the coherence length of the magnetic field, and this relation is understood to apply when $\lambda_{\rm coh}$ is smaller than the cooling length for GeV production.) For PKS 2155-304, therefore, the rapidly varying VHE gamma-ray fluxes during the summer 2006 TeV flares must originate from photons produced near the source.

This conclusion does not hold, however, for a fraction of blazars and radio galaxies from which prominent variability has not been seen. For example, weakly variable emissions in Mrk 501 and Mrk 421 at GeV energies could arise from variable TeV source photons cascading in the weak IGMF (Neronov et al. 2011). Another interesting source is 1ES 0229+200, which has a hard VHE component, but has not been reported to be variable in observations taken over a period of 3 – 4 yr (Aharonian et al. 2007b; Perkins et al. 2010). The highly variable VHE radiation from such extreme TeV blazars could either be leptonic synchrotron/Compton, or proton synchrotron or photohadronic cascade radiation, whereas the less variable component could be emitted from an extended jet. In addition to these possibilities of emissions produced in the source, there are not only gamma-ray-induced cascade emission but also proton-induced cascade emission, i.e., intergalactic cascades caused by UHE gamma rays and pairs generated via the photomeson production with the CMB and EBL. Such cascade emission, which should be weakly or non-variable, may confuse interpretation of the minimum bulk Lorentz factor from $\gamma\gamma$ opacity arguments and the level of the EBL (Essey et al. 2010; Essey et al. 2011).

Here we focus on the intergalactic cascade emission to explain hard VHE spectra of extreme TeV blazars whose variability is apparently weak or absent. We calculate the cascade emission by solving the Boltzmann equations, where $\gamma\gamma$ pair creation, IC scattering, synchrotron radiation, and adiabatic energy loss are taken into account (Lee 1998; Murase & Beacom 2011). As for proton propagation, we directly solve the equation of motion of protons one by one, with photomeson production simulated by SOPHIA (Mücke et al. 2000) and the Bethe-Heitler process included to treat interactions with the ambient photon field. Then the electromagnetic cascade is calculated separately. For the EBL model, we employ the low-IR and best-fit models (Kneiske et al. 2004; Kneiske & Dole 2010, see Finke et al. 2011 for detailed discussions on the EBL). We focus

on the possibility that the cascade interpretation is a viable explanation of VHE gamma-ray spectra of extreme TeV blazars, where we require that the IGMF in voids is so weak that the cascade flux suppression at TeV energies due to the IGMF is small as long as $B_{\rm IG}\lambda_{\rm coh}^{1/2} \lesssim 10^{-15}$ G Mpc$^{1/2}$ (e.g., Dolag et al. 2011; Tavecchio et al. 2011; Taylor et al. 2011; Ahlers & Salvado 2011). On the other hand, as noted above, we implicitly require that the IGMF be not too weak due to constraints from *Fermi*.

An important point is that cosmic magnetic fields are almost certainly inhomogeneous. Whereas one may expect very weak IGMFs in voids, $B_{\rm IG}\lambda_{\rm coh}^{1/2} \ll 10^{-9}$ G Mpc$^{1/2}$, the structured region of the universe is likely to be significantly magnetized. Clusters of galaxies are known to have $B_{\rm EG} \sim 0.1-1$ μG (e.g., Vallée 2004), and recent simulations have suggested that filaments have $B_{\rm EG} \sim 1-10$ nG (Ryu et al. 2008; Das et al. 2008, and see also, e.g., Donnert et al. 2009), which are larger than levels expected for the IGMF in voids, and galaxies including AGN are likely located in these structured region of the universe. The mean free path of $\lesssim$ 100 TeV and $\gtrsim$ 3 EeV gamma rays is larger than $\sim$ Mpc (e.g., Dermer 2007), so that one may expect that the cascade emission induced by VHE/UHE primary gamma rays is primarily developed in the voids. On the other hand, ions must propagate in the clusters and/or filaments, so that they are deflected (and delayed) by their magnetic fields. Indeed, as demonstrated by a number of authors, the structured EGMFs play a crucial role on propagation of UHECRs (e.g., Takami et al. 2006; Das et al. 2008), and this is even more so the case for lower-energy cosmic rays.

3.1. *Cascades by Primary VHE/UHE Gamma Rays*

SEDs of typical TeV blazars are generally well reproduced by the standard one-zone electronic synchrotron/SSC model. Extreme TeV blazars have hard VHE gamma-ray spectra, which are often indicated by lower-energy optical-UV/X-ray fluxes, or from GeV gamma-ray data provided by *Fermi*. But it is not easy to have such hard gamma-ray spectra at $\sim 1-10$ TeV energies as indicated by deabsorption of the measured gamma-ray spectrum based on conventional EBL models (discussed below). One of the reasons is that unusually large values of $\delta \sim 10^2-10^3$ are often needed to avoid the Klein-Nishina suppression. For 1ES 0229+200, PKS 0548-322 and 1ES 0347-121, extreme values of the electron minimum Lorentz factor of $\gamma_{e,m} \sim 10^4-10^5$ are required from spectral modeling, where the hard SSC spectrum, $F_E \propto E^{-2/3}$ (in the Thomson regime) can be expected in the VHE range (Tavecchio et al. 2011).

There are several alternate blazar models that predict very hard $\sim 30-100$ TeV gamma-ray emission. In the hadronic model, the proton synchrotron process leads to multi-TeV emission if the outflow is ultra-relativistic, $\Gamma \sim 10^2-10^3$. Then, further hardening may be caused by the internal absorption due to some soft photon field outside the blob (Zacharopoulou et al. 2011). Another possibility to make hard TeV emission is electromagnetic radiation produced by nonthermal electrons in the vacuum gap of the black hole magnetosphere (e.g., Levinson 2000).

Another type of model predicts very weak variability. Böttcher et al. (2008) suggested that hard VHE emission originates from relativistic electrons accelerated in the extended jet Compton-scatters CMB photons. In this model, if the electron spectrum is hard, $p \sim 1.5$, the resulting IC photon number

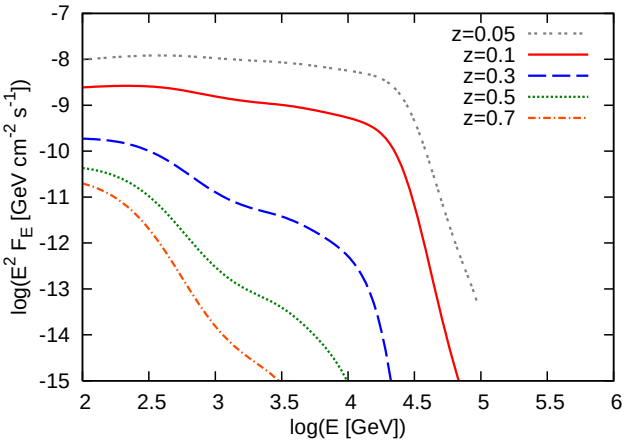

FIG. 1.— Spectra of VHE gamma-ray-induced cascade emission for various source redshifts. We assume the total gamma-ray luminosity of $L_\gamma = 10^{45}$ erg s^{-1} with $\beta = 2/3$ and $E^{\rm max} = 100$ TeV. The low-IR EBL model of Kneiske et al. (2004) is used here.

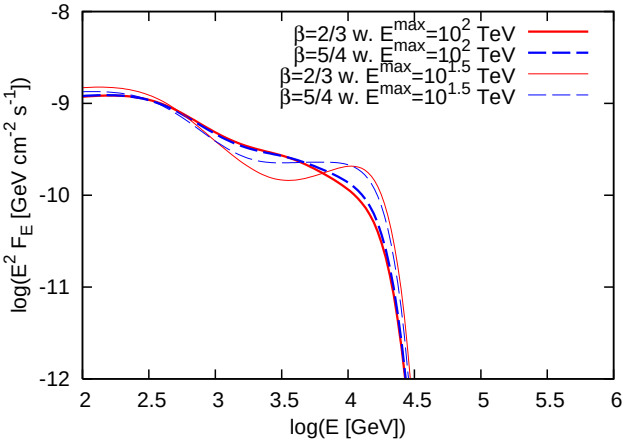

FIG. 2.— Spectra of VHE gamma-ray-induced cascade emission for various intrinsic photon spectra. The source redshift is set to $z = 0.14$.

spectrum becomes $F_E \propto E^{-(1+p)/2} \sim E^{-5/4}$ that can be compatible with the observed VHE gamma-ray spectrum. The same process could be important for recollimation shocks or acceleration at knots and hotspots.

When VHE gamma rays are emitted from a source, they induce an electromagnetic cascade in intergalactic space. This cascade unavoidably accompanies spectral production of extreme TeV blazars as long as the IGMF in voids is weak enough. To demonstrate this, we show in Figures 1 and 2 the VHE gamma-ray-induced cascade emission for sources at various redshifts. In Figure 1, primary source photons with $F_E \propto E^{-\beta}$ with $\beta = 2/3$ and $E^{\rm max} = 100$ TeV are assumed. In Figure 1, one sees that the observed cutoff due to the EBL becomes lower for more distant sources since the $\gamma\gamma$ pair-creation opacity increases. In Figure 2, a different photon index ($\beta = 5/4$) and/or a different maximum energy ($E^{\rm max} = 10^{1.5}$ TeV) are assumed for comparison, which causes slight differences in spectra.

Another way to have gamma-ray induced emission involves UHE gamma rays produced in blazar jets or radio galaxies. Such a case is shown in Figure 3 assuming much higher injected photon energies, within 1/2 decade centered at

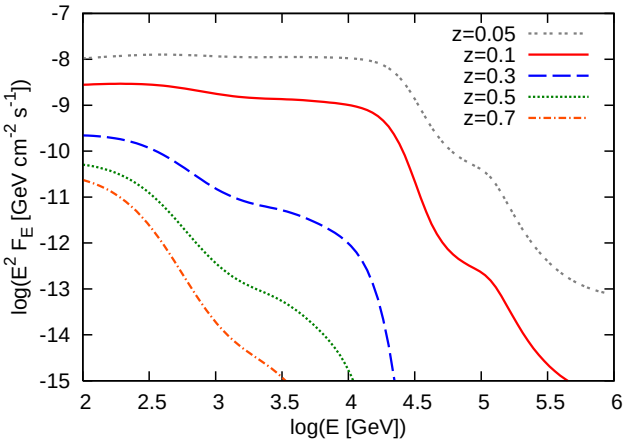

FIG. 3.— Spectra of UHE gamma-ray-induced cascade emission for various source redshifts. We assume $L_\gamma = 10^{45}$ erg s^{-1} at $10^{18.75}-10^{19.25}$ eV.

10 EeV. The photomeson production by UHE protons, which can be expected in hadronic models, leads to $E_\gamma \approx 0.1E_p \simeq 10^{19}$ eV $E_{p,20}$ photons. In the synchrotron source in which UHE protons are accelerated, one may expect the synchrotron self-absorption cutoff, where UHE photons may escape from the emission region (Murase 2009). A caveat of this model in our case is that generation of UHE gamma rays in the source require acceleration of UHE protons and efficient photomeson production in the source. As noted before, the photomeson production in the source will not be so efficient in high-peaked BL Lac objects, which implies that the required UHECR luminosity has to be very large. As can be seen, there is some notable differences at low redshifts $z \lesssim 0.1$ due to the longer effective energy loss length of UHE gamma rays, but the received spectra are not strongly sensitive to the energy at which the photons are injected for higher redshift sources.

Note that in the intergalactic cascade scenario, we do not expect strong fluxes with fast time variability, though some variable contributions may come from the gamma-ray emission component made at the source. Although there is no strong evidence of time variability for several extreme TeV blazars, future observations by CTA (CTA Consortium 2010), HAWC (Sandoval et al. 2009), LHAASO (Cao 2010), or SCORE (Hampf et al. 2011) will be crucial for distinguishing between the models.

3.2. *Cascades by Primary UHECRs*

In the previous subsection, we considered cascade emission induced by primary gamma rays. VHE gamma rays at sufficiently low energies, or UHE gamma rays with energies $\gg 10^{15}$ eV, where the opacity of the background radiation is not so large, can leave the structured region of the universe, whereas cosmic rays should feel structured EGMFs in clusters and filaments. The deflection of cosmic rays by the structured region with the size of $l \sim$ Mpc and the regular magnetic field of $B_{\rm EG} \sim 10$ nG (which may be typical of filaments; Ryu et al. 2008) is estimated to be

$$\theta_B \approx \frac{\sqrt{\lambda_{\rm coh} l}}{r_L} \simeq 17^\circ\, Z E_{A,19}^{-1} B_{\rm EG,-8} \left(\frac{\lambda_{\rm coh}}{0.1\ {\rm Mpc}}\right)^{1/2} \left(\frac{l}{\rm Mpc}\right)^{1/2}. \quad (7)$$

Therefore, the deflection by the structured EGMFs is not negligible for cosmic rays below $\sim 10^{19}$ eV, since the deflection angle is larger than the typical jet opening angle of $\theta_j \sim 0.1 \sim 6^\circ$.

In order to model the structured EGMFs, we have assumed a simplified two-zone model with structured EGMF and IGMF in voids (see H. Takami & K. Murase 2011, in preparation, for details). We model a cluster of galaxies by a sphere with the radius of 3 Mpc, and $B_{\rm EG}(r) = B_0(1+r/r_c)^{-0.7}$, with $B_0 = 1$ μG and $r_c = 378$ kpc. The magnetic field direction is assumed to be turbulent with the Kolmogorov spectrum and the coherent length of $\lambda_{\rm coh} = 100$ kpc. In addition to the EBL, the infrared background in the cluster is considered as the superposition of the SEDs of 100 giant elliptical galaxies calculated by GRASIL (Silva et al. 1998), using fitting formula for the gas distribution (Rordorf et al. 2004). Filaments are modeled by a cylinder with a radius of 2 Mpc (Ryu et al. 2008) and a height of 25 Mpc. The magnetic field is assumed to be turbulent, which is described by the Kolmogorov spectrum with $B_{\rm EG} = 10$ nG and $\lambda_{\rm coh} = 100$ kpc, although these values are very uncertain. Some numerical simulations imply a large-scale coherent component of the magnetic field in filaments (e.g., Brüggen et al. 2005), which may deflect cosmic-ray trajectories more efficiently. UHECRs are injected from the center of the filament toward a direction perpendicular to the cylindrical axis to see the relatively conservative case. Throughout this work, the IGMF in voids is assumed to be weak enough to be less important for cosmic-ray deflections.

In Figure 4, we show our numerical results for the case $E_p^{\rm max} = 10^{19}$ eV expected in the standard synchrotron/SSC model of typical, variable BL Lac objects and FR-I galaxies. One sees that the structured EGMFs play an important role by suppressing the resulting gamma-ray flux by more than one order of magnitude compared to the case without them. In Figure 5, we show the case of $E_p^{\rm max} = 10^{20}$ eV, which can be achieved in the hadronic model. While the Bethe-Heitler pair-creation process dominantly provides an electromagnetic component in Figure 4, contribution of photomeson production is more important in Figure 5. In the filament case, the deflection angle of UHECRs around 10^{20} eV is still less than the jet opening angle, so that the gamma-ray flux is diluted by only a small factor. On the other hand, in the cluster case, because UHECRs cannot be beamed, the gamma-ray flux becomes almost isotropic and the corresponding flux is reduced according to the jet beaming factor $(1-\cos\theta_j) \simeq 1/200$ for $\theta_j = 0.1$. The effects of the structured EGMFs are illustrated in Figure 6, where the relative contributions are calculated from two-dimensional Gaussian fits. Note that if we express the isotropic cosmic-ray luminosity where cosmic rays leave the structured region as $EL_E^{\rm CR,iso}$, then the relative contributions are $(1-\cos\theta_j)(EL_E^{\rm CR,iso})/(EL_E^{\rm CR,}{}^j)$. In the filament case, isotropization becomes significant at $\sim 10^{19}$ eV rather than at $\sim 10^{21}$ eV for the cluster case.

In Figure 7, we show resulting gamma-ray spectra for various redshifts. Owing to the Bethe-Heitler process with energy-loss length $\sim$ Gpc, UHE protons continue to supply electron-positron pairs for a longer distance than the photomeson energy loss length of ~ 100 Mpc. As a result, the dependence of the proton-induced gamma-ray fluxes on distance is much gentler than gamma-ray-induced fluxes. Indeed, one sees that the relative importance of the proton-induced gamma-ray flux to the gamma-ray induced flux increases with distance (compare Figure 7 with Figures 1 and 3). Importantly for distant sources, the proton-induced cas-

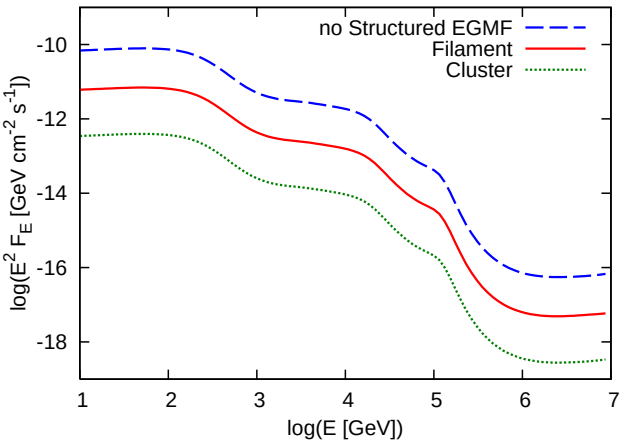

FIG. 4.— Effects of the structured EGMF on the gamma-ray flux. We assume $L_{\rm CR} = 10^{45}$ erg s^{-1}, with $E_p^{\rm max} = 10^{19}$ eV and $p = 2$. Here, as in the results on cascade emission induced by primary gamma rays, we use the isotropic cosmic-ray luminosity at the source (but above $10^{18.5}$ eV), which is related to the beaming-corrected cosmic-ray luminosity, $L_{{\rm CR},j}$, as $L_{\rm CR} \equiv (1-\cos\theta_j)^{-1} L_{{\rm CR},j}$. Here the assumed jet opening angle $\theta_j = 0.1$. The source redshift is set to $z = 0.5$.

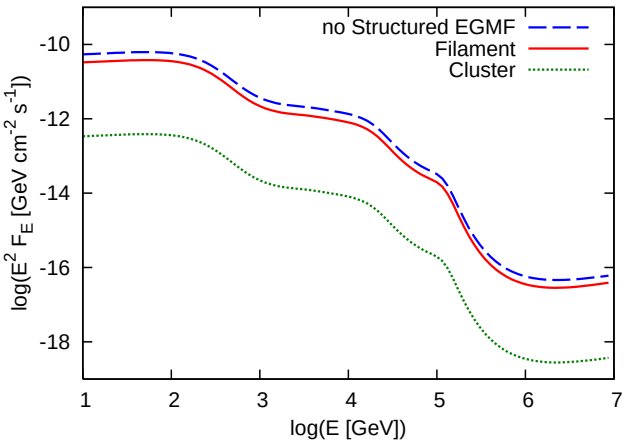

FIG. 5.— Same as Figure 4, but with $E_p^{\rm max} = 10^{20}$ eV.

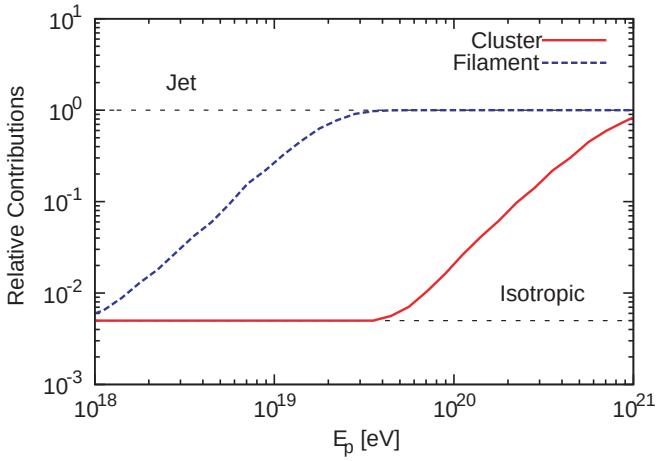

FIG. 6.— Effects of the structured EGMFs on the deflection of UHE protons. Relative contributions represent how much the apparent cosmic-luminosity is diluted from $L_{\rm CR}$, where cosmic rays enter the void region. Note that a two-sided jet is considered throughout this work.

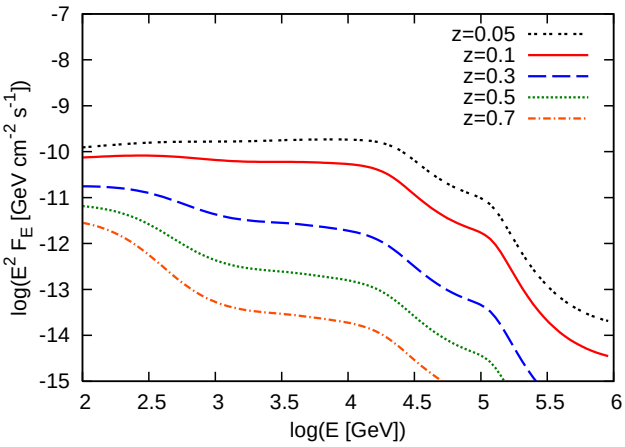

FIG. 7.— Spectra of UHE proton-induced cascade emission for various source redshifts. We assume $L_{\rm CR} = 10^{45}$ erg s^{-1} with $E_p^{\rm max} = 10^{19}$ eV and $p = 2$. The source is assumed to be located in the filament with $B_{\rm EG} = 10$ nG and $\lambda_{\rm coh} = 0.1$ Mpc. The low-IR EBL model is here assumed.

cade spectrum is much harder than the gamma-ray induced spectrum, especially above TeV energies. Future VHE observations by CTA and HAWC are important to identify the origin of UHECRs through detection of high-energy γ rays, as we now demonstrate for 1ES 0229+200 in the next subsection.

In this work, we are interested in cases where IC cascade emission in voids is important in the VHE range, since it can explain hard VHE spectra of extreme TeV blazars as suggested by Essey et al. (2010). One should also keep in mind that the proton-induced GeV-TeV synchrotron emission from the structured region itself, where the EGMFs are stronger, should also be expected (see Gabici & Aharonian 2005; Kotera et al. 2009; Kotera et al. 2011, and references therein), though it is not viable as an explanation of the hard spectra of extreme TeV blazars. For a weak IGMF that is of interest in this work, its relative importance is somewhat smaller when the volume filling fraction of the magnetized region is taken into account.

We have demonstrated the likely importance of the structured EGMFs for proton-induced intergalactic cascade emission. They are also important for UHE nuclei. Since nuclei with energy ZE_p have the same deflection angle as protons with energy E_p, our results indicate that Fe nuclei should be significantly isotropized for all observed UHECR energies. For UHE nuclei, the photodisintegration energy loss length is ~ 100 Mpc, for which the energy fraction carried by gamma rays and neutrinos is small as long as $E_A^{\rm max}$ is not too high. On the other hand, UHE nuclei supply high-energy pairs via the Bethe-Heitler process, whose effective cross section is $\kappa_{{\rm BH},A}\sigma_{{\rm BH},A} \sim \kappa_{{\rm BH},p}\sigma_{{\rm BH},p}(Z^2/A)$, which induces cascades in the same manner as UHE protons.

3.3. *Implications for TeV-PeV Observations*

In a wide range of EBL models, deabsorption of measured TeV blazar spectra leads to hard excesses at $>$TeV energies in, e.g., 1ES 1101-232, 1ES 0229+200, and 1ES 0347-121 (see, e.g., Fig. 8 in Finke et al. 2010). TeV excesses are also seen above the extrapolation of the GeV flux from NGC 1275 (Abdo et al. 2009b) and the core of Cen A (Abdo et al. 2010d). These unusual TeV spectral emission

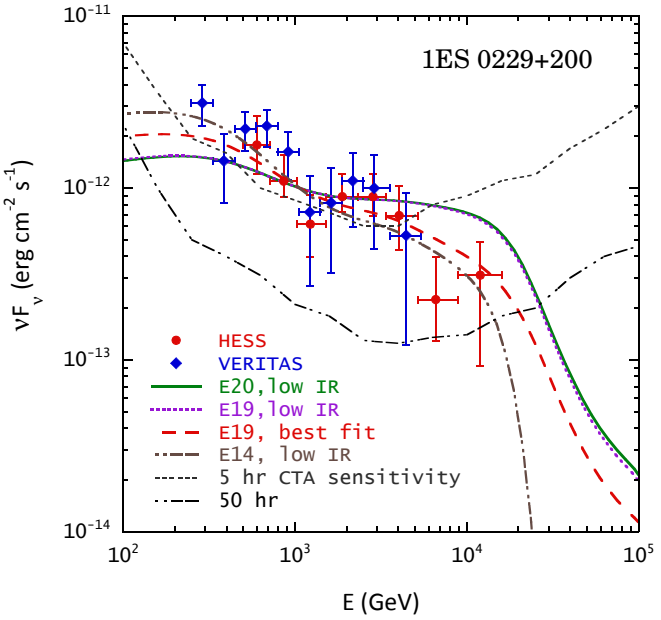

FIG. 8.— Spectral fits to HESS and VERITAS data of 1ES 0229+200. Blue data points are from HESS (Aharonian et al. 2007b), and red data points are preliminary VERITAS data (Perkins et al. 2010). The curves labeled "E20, low IR" and "E19, low IR" are the cascade spectra initiated by the E^{-2} injection with $E_p^{\rm max} = 10^{20}$ eV and 10^{19} eV protons, respectively, using the low-IR EBL model (Kneiske et al. 2004), whereas the curve labeled "E19, best fit" is the spectrum with $E_p^{\rm max} = 10^{19}$ eV for the best-fit EBL model. The curve labeled "E14, low IR" is the spectrum resulting from the cascade of $E^{\rm max} = 10^{14}$ eV photons with $\beta = 5/4$ produced at the source for the low-IR EBL model. Double dot-dashed and dotted curves give, respectively, the 5 sigma differential sensitivity for 5 and 50 hr observations with CTA (configuration E; CTA Consortium 2010).

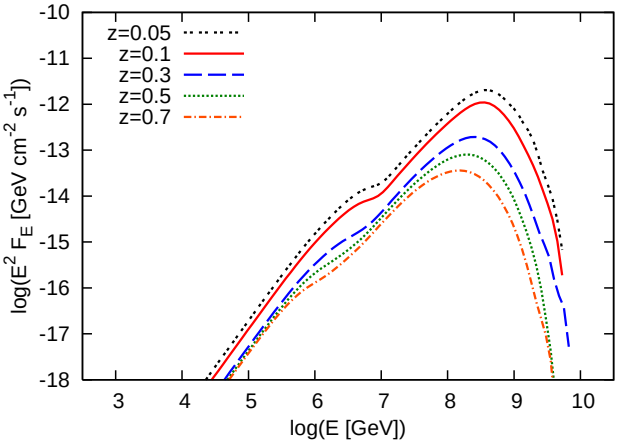

FIG. 9.— Spectra of UHE proton-induced neutrino emission for various source redshifts. The parameters used here are the same as Figure 7.

components are conventionally explained by emissions at the source. But they could also be explained by intergalactic cascade emissions.

Figure 8 demonstrates that 1ES 0229+200 can be fit by both the gamma-ray induced cascade and proton-induced cascade emissions. Because of the uncertainty in the EBL models, it is not easy to distinguish between the two possibilities at ~ 100 GeV – TeV energies. At higher energies, however, our calculations show that it is possible to discriminate a proton-induced cascade emission from gamma-ray-induced cascade emission resulting from the attenuation of hard gamma-ray source emission. The emission spectrum measured as a result of the injection of VHE photons at the source are strongly suppressed above ~ 10 TeV for a wide range of EBL models, whereas a cosmic-ray-induced cascade displays a significantly harder spectrum above this energy. Because UHE photons and pairs can only be produced as secondaries of hadronic processes, then cascades from UHE protons demonstrate that a distant blazar is an UHECR source, which provides another test other than gamma-ray variability searches that are critical for discriminations among the scenarios.

Figure 8 indicates that detection of > 25 TeV gamma rays is only compatible with a hadronic origin. Identifying this feature by future Cherenkov detectors such as CTA or HAWC makes possible the gamma-ray demonstration of the sources of UHECRs, and we show the differential sensitivity goal of the planned imaging atmospheric Cherenkov telescope, CTA (CTA Consortium 2010). Note that this is a differential sensitivity curve with the requirement of 5 sigma significance for 50 hour observations per bin, with 4 bins per decade. This is a much more stringent requirement than detection of a source with 5 sigma based on integrated flux, which can be divided into 3 data points with ≈ 3 sigma significance each. Given the differential CTA sensitivity for a 50 hr observation, the spectral hardening associated with hadronic cascade development can be clearly detected.

It is theoretically expected that discriminating between cosmic-ray–induced and gamma-ray–induced cascade emissions may be easier for higher redshift sources. For the gamma-ray-induced cascade, there should be a cutoff because of the $\gamma\gamma$ pair creation by the EBL, while spectra of the cosmic-ray-induced cascade emission are kept hard because of the continuous injection by the Bethe-Heitler process. Hence, deep observations at $\gtrsim$ TeV energies by CTA or HAWC for moderately high-redshift blazars will also be important to resolve this question, along with detailed theoretical calculations for individual TeV blazars.

Now that IceCube has been completed, along with VHE gamma-ray data and GeV observations with the *Fermi* satellite, it has started to give important insights into the origin of UHECRs. But detection of neutrino signals produced outside the source seems difficult for high-peaked BL Lac objects and FR-I galaxies, because the point source flux sensitivity at > 10 PeV is order of $\sim 10^{-11}$ GeV cm^{-2} s^{-1} (Spiering 2011), which is typically larger than the expected neutrino fluxes, as shown in Figure 9. On the other hand, the diffuse background neutrino flux would be detectable especially for $E_p^{\rm max} \gtrsim 10^{20}$ eV (e.g., Anchordoqui et al. 2007; Takami et al. 2009, and references therein), which is possible in hadronic models with large magnetic fields in jets. For $E_p^{\rm max} = 10^{19}$ eV, however, protons mostly interact with the EBL, and the expected flux is lower than the proton case even if nuclei can be accelerated up to $E_A = ZE_p$ (e.g., Anchordoqui et al. 2007). If BL Lac objects and FR-I galaxies are the main sources of UHECRs made mainly of ions with $E_A \lesssim Z10^{19}$ eV, the diffuse neutrino background would be difficult to be detected by IceCube.

Next, let us discuss the cosmic-ray luminosity required to explain such extreme TeV blazars in the hadronic cascade scenario. Our calculations in Figure 8 show that less power is required for a cosmic-ray induced cascade than a

photon-induced cascade. If no structured EGMFs are there, the required isotropic cosmic-ray luminosity (at the source) is $L_{\rm CR} \sim 10^{45}-10^{46}$ erg s^{-1}, which is consistent with Essey et al. (2011), Razzaque et al. (2011), and the calculation for 1ES 0229+200 shown here. It is also consistent with the proton power needed in hadronic models for typical BL Lac objects. Note that the corresponding beaming-corrected cosmic-ray luminosity is $L_{{\rm CR},j} \sim 10^{43}$ erg s^{-1}. Where the structured EGMFs play a role, however, the required isotropic cosmic-ray luminosity (at the source) is much larger. We obtained $L_{\rm CR} \sim 10^{46}-10^{47}$ erg s^{-1} (for filaments) and $L_{\rm CR} \sim 10^{47}-10^{48}$ erg s^{-1} (for clusters), depending on the EBL model and spectral indices, when we assume $E_p^{\rm max} = 10^{19}$ eV that is expected in the standard synchrotron/SSC model. (In Figure 8, the inferred isotropic luminosities are $L_{\rm CR} \simeq 10^{46}$ erg s^{-1} (for the filament) and $L_{\rm CR} \simeq 5\times10^{46}$ erg s^{-1} (for the cluster), respectively, while $L_\gamma \simeq 10^{45}$ erg s^{-1} when primary gamma rays are injected.) As discussed below, such cosmic-ray luminosities seem a bit extreme, so that models with strong magnetic fields in inner jets are favored if we adopt the hadronic cascade interpretation of those extreme TeV blazars.

It is useful to compare those luminosities with the required UHECR energy budget indicated from UHECR observations. From recent PAO observations, the local UHECR energy budget above $10^{18.5}$ eV is a few $\times10^{44}$ erg Mpc^{-3} yr^{-1}. For the local blazar density, $n_s \sim 10^{-6.5}$ Mpc^{-3} (Padovani & Urry 1990), the inferred isotropic UHECR luminosity of $L_{\rm CR} \sim 10^{43.5}$ erg s^{-1} (regarding blazars as AGN pointing toward us). This is smaller than the cosmic-ray luminosity required for explaining extreme TeV blazars, which implies that those distant AGN with hard VHE spectra should be rarer and more powerful in cosmic rays than nearby AGN responsible for the observed UHECRs. For 1ES 0229+200, the single-source flux is ~ 10 % of the observed UHECR flux so that the anisotropy could be used as a useful probe. Also, models with strong magnetic fields, as in the hadronic models for typical TeV blazars, are preferred compared to the one-zone SSC model.

We demonstrated the importance of structured EGMFs that help isotropize the trajectories of UHECRs, though the EGMF strengths are still uncertain. There are other causes that can diminish the beaming of UHECRs and resulting cascade fluxes. One is the cosmic-ray streaming instability which might amplify the IGMF up to $\gg 10^{-15}$ G (K. Murase et al. 2011, in preparation). Radio lobes of AGN, like in the case of Cen A with $B \sim 1$ μG, would also isotropize UHECRs (Dermer et al. 2009), as might radio bubbles from the jets of radio galaxies. These magnetic fields allow cosmic rays from jets of FR-I galaxies to contribute to the observed flux of UHECRs. Indeed, for nearby AGN, the UHECRs must be significantly deflected, since there is no evidence of cross-correlation with nearby blazars such as Mrk 501 and Mrk 421 (Dermer et al. 2009). Also, UHECR sources with $L_{\rm CR} \gtrsim 10^{45}$ erg s^{-1} at ~ 100 Mpc will lead to overshooting the observed UHECR spectral flux. It is also supported by analyses of auto-correlation, which indicate that the UHECR source density is larger than $n_s \sim 10^{-5}$ Mpc^{-3} in the proton-dominated composition case (Kashti & Waxman 2008; Takami & Sato 2009). Relating the local UHECR source density with the local FR-I galaxy density, $n_s \sim 10^{-4}$ Mpc^{-3} (e.g., Padovani & Urry 1990), then the inferred UHECR luminosity is typically $L_{{\rm CR},j} \sim 10^{41}$ erg s^{-1}.

4. DISCUSSION AND SUMMARY

In this work we studied BL Lac objects and FR-I radio galaxies as potential UHECR sources in light of recent *Fermi* and imaging atmospheric Cherenkov telescope observations, and considered how future CTA, HAWC, and other high-energy gamma-ray experiments might test the origin of the gamma rays from this class of blazars.

If one accepts the standard synchrotron/SSC model for typical, variable BL Lac objects and FR-I galaxies that comprise the majority of VHE blazars, the proton maximum energy is typically $\sim 1-10$ EeV, and only heavier nuclei reach the highest energies. In terms of maximum energy, a heavy-ion dominated composition can be compatible with the standard SSC model because Fe nuclei can be accelerated to $\gtrsim 10^{20.5}$ eV while surviving against photodisintegration (if $\delta \gtrsim 20$; see equation 6). An open issue of the heavy-ion dominated composition scenario of AGN is how the significant amount of heavy nuclei is loaded in jets, which is suggested from the PAO composition results and the observed isotropy in arrival distribution at $\sim 10^{19}$ eV $Z_{1.5}^{-1}E_{A,20.5}$.

Extreme TeV blazars such as 1ES 0229+200 could be explained by gamma rays that are produced via the electronic SSC process in inner jets, but hard EBL-deabsorbed VHE spectra typically lead to extreme source parameters (Tavecchio et al. 2011). Alternative interpretations by gamma-ray-induced or proton-induced cascaded emissions are possible for weakly variable of non-variable sources, provided that the IGMF is weak enough. We examined these possibilities with numerical calculations, taking into account effects of structured EGMFs in filaments and clusters, and demonstrated that structured EGMFs would play an important role on the proton-induced cascade emission, and that cosmic rays are significantly isotropized especially for the maximum proton energy of ~ 10 EeV. In this case, rather large cosmic-ray luminosities are required in order to explain the emission from extreme TeV blazars such as 1ES 0229+200 by the cascade radiation induced by UHECRs.

If hadronic models are adopted for typical BL Lac objects and FR-I galaxies, then the observed VHE emission from these objects could be proton synchrotron radiation if protons are accelerated up to $\sim 10^{20.5}$ eV, which requires strong magnetic fields, $B' \sim 10-100$ G, that could be achieved in the inner jets of the blazars. Such hadronic models can be compatible with a proton-dominated composition. Especially for luminous blazars, including spectacular flares and low-peaked BL Lac objects with scattered radiation fields in the broad line region, one may expect high-energy neutrinos produced in inner jets as one of the hadronic signatures (e.g., Atoyan & Dermer 2001).

Protons with energy $E_p^{\rm max} \sim 10^{20}$ eV can avoid strong deflections in the structured region, and the required cosmic-ray luminosity to power VHE emission from extreme TeV blazars seems reasonable, though UHECR observations suggest that UHECRs must be significantly isotropized at least for nearby AGN and those distant blazars should be more powerful in cosmic rays than such nearby AGN that are responsible for the observed UHECR spectrum.

It should be crucial to make observational tests on the origin of extreme TeV blazars such as 1ES 0229+200 to reveal the radiation mechanism of BL Lac objects and FR-I galaxies and obtain a clue to the UHECR acceleration, de-

spite the above potential issues. Future variability searches with CTA will be important. In addition, discrimination of the proton-induced intergalactic cascade from the gamma-ray-induced cascade and attenuated source emission is possible from measurements at $\gtrsim 1-10$ TeV energies. Detection of high-energy photons above 25 TeV from 1ES 0229+200 or above $\sim$ TeV from more distant blazars, which may be realized by future gamma-ray detectors such as CTA and HAWC, would be compelling evidence that this kind of object is a source of UHECRs. In addition to gamma-ray observations, the anisotropy search with UHECRs could be helpful, though it depends on the local EGMF strength.

In this work we focused on UHECR acceleration in the inner jets of BL Lac objects and FR-I galaxies. Note that FSRQs and FR-II galaxies are rarer but more powerful, and they should also be sources of UHECRs and neutrinos. Other scenarios such as shock acceleration at hot spots (e.g., Takahara 1990; Rachen & Biermann 1993; Takami & Horiuchi 2011) and cocoon shocks (e.g., Norman et al. 1995; Ohira et al. 2010) are viable for these types of AGN. But their local number density, $n_s \sim 10^{-7.5}$ Mpc^{-3}, appears to be too small in the proton-dominated case to avoid strong anisotropy in the local universe (Takami & Sato 2009). In the heavy-ion dominated composition case, not only blazars and radio galaxies, but also radio-quiet AGN (Pe'er et al. 2009) could be sources of UHE nuclei.

In summary, we have considered observational implications of BL Lac objects and FR-I galaxies as sources of UHECRs. Within the standard synchrotron SSC model, acceleration of UHE protons to energies $\gtrsim 10^{19}$ eV is unlikely, so the composition of higher-energy cosmic rays should be dominated by ions within the framework of this model. The intergalactic cascade emission has to be small for highly variable blazars and radio galaxies, while it can play a role on the spectrum of weakly variable or non-variable objects, especially extreme TeV blazars. If the TeV spectrum of those blazars is produced by cascade emission by UHE protons, then magnetic fields in the structured regions can significantly isotropize protons, increasing the luminosity demands on these sources. The cascade emissions induced by VHE photons and UHE protons can be distinguished by future multi-TeV observations from CTA and HAWC. In particular, detection of $\gtrsim 25$ TeV photons from relatively low-redshift sources such as 1ES 0229+200 or $\gtrsim$ TeV photons from more distant sources would favor such objects as being sources of UHECRs.

K.M. acknowledges financial support by a Grant-in-Aid from JSPS, from CCAPP and from NRL. The work of C.D. is supported by the Office of Naval Research and NASA Fermi Guest Investigator grants. We thank John Beacom, Adrian Biland, Gernot Maier, and Soebur Razzaque for discussions.

REFERENCES

Abbasi, R. U. 2010, et al., Phys. Rev. Lett. 104, 161101
Abraham, J., et al. 2008, Astropart. Phys., 29, 188
Abraham, J., et al., arXiv:0906.2189.
Abraham, J., et al. 2010, Phys. Rev. Lett. 104, 091101
Abdo, A. A., et al. 2009a, ApJ, 707, L142 (RLNLSy1)
Abdo, A. A., et al. 2009b, ApJ, 699, 31 (NGC 1275)
Abdo, A. A., et al. 2009c, ApJ, 707, 55 (M87)
Abdo, A. A., et al. 2010a, ApJ, 715, 429 (1LAC)
Abdo, A. A., et al. 2010b, ApJ, 709, L152 (starburst)
Abdo, A. A., et al. 2010c, ApJ, 720, 912 (MAGN)
Abdo, A. A., et al. 2010d, ApJ, 719, 1433 (Cen A)
Abdo, A. A., et al. 2011a, ApJ, 726, 43, (e) 731, 77 (3C 66A)
Abdo, A. A., et al. 2011b, ApJ, 730, 101 (BL Lac)
Abdo, A. A., et al. 2011c, ApJ, 727, 129
Abreu, P., et al. 2011, arXiv:1106.3048
Acciari, V.A., et al. 2009, ApJ, 707, 612
Acciari, V.A., et al. 2011, ApJ, 729, 2
Aharonian, F., et al. 2007a, ApJ, 664, L71 (PKS 2155-304)
Aharonian, F., et al. 2007b, A&A, 475, L9 (1ES 0229+200)
Aharonian, F., et al. 2007c, A&A, 470, 475 (1ES 1101-232)
Aharonian, F. A., Coppi, P. S., & Völk, H. J. 1994, ApJ, 423, L5
Aharonian, F. A. 2000, New Astronomy, 5, 377
Aharonian, F. A., et al. 2009, A&A, 502, 749
Ahlers, M., & Salvado, J. 2011, arXiv:1105.5113
Albert, J., et al. 2007, ApJ, 669, 862 (Mrk 501)
Aleksić, J., et al. 2010, ApJ, 723, L207 (IC 310)
Aleksić, J., et al. 2011a, A&A, 530, A4 (3C 279)
Aleksić, J., et al. 2011b, ApJ, 730, L8 (PKS 1222+21)
Anchordoqui, L. A., et al. 2007, Phys. Rev. D, 76, 123008
Anderhub, H., Antonelli, L. A., Antoranz, P., Backes, M., Baixeras, C., Balestra, S. 2009, ApJ, 705,1624
Arons, J. 2003, ApJ, 589, 871
Atoyan, A., & Dermer, C. D. 2001, Phys. Rev. Lett., 87, 221102
Begelman, M. C., Fabian, A. C., & Rees, M. J. 2008, MNRAS, 384, L19
Berezinsky, V., Gazizov, A. Z., & Grigorieva, S. I. 2002, arXiv:astro-ph/0210095
Berezinsky, V., Gazizov, A., & Grigorieva, S. 2006, Phys. Rev. D, 74, 043005
Boldt, E., & Ghosh, P. 1999, MNRAS, 307, 491
Böttcher, M., Dermer, C. D., & Finke, J. D. 2008, ApJ, 679, L9
Brüggen, M., et al. 2005, ApJ, 631, L21
Cao, Z., 2010, Chinese Physics C, 34, 249
CTA Consortium 2010, arXiv:1008.3703
Das, S., Kang, H., Ryu, D., & Cho, J. 2008, ApJ, 682, 29
Dermer, C. D. 2007, arXiv:0711.2804
Dermer, C. D., & Razzaque, S. 2010, ApJ, 724, 1366
Dermer, C. D., Razzaque, S., Finke, J. D., & Atoyan, A. 2009, New J. Phys., 11, 065016
Dermer, C. D., Cavadini, M., Razzaque, S., Finke, J. D., Chiang, J., & Lott, B. 2011, ApJ, 733, L21
Dolag, K., Kachelriess, M., Ostapchenko, S., & Tomàs, R. 2011, ApJ, 727, L4
Donnert, J., Dolag, K., Lesch, H., & Müller, E. 2009, MNRAS, 392, 1008
Essey, W., Kalashev, O. E., Kusenko, A., & Beacom, J. F. 2010, Phys. Rev. Lett., 104, 141102
Essey, W., Kalashev, O., Kusenko, A., & Beacom, J. F. 2011, ApJ, 731, 51
Finke, J. D., Dermer, C. D., Böttcher, M. 2008, ApJ, 686, 181
Finke, J. D., Razzaque, S., & Dermer, C. D. 2010, ApJ, 712, 238
Fossati, G., et al. 2008, ApJ, 677, 906 (Mrk 421)
Gabici, S., & Aharonian, F. A. 2005, Phys. Rev. Lett., 95, 251102
Ghisellini, G., Maraschi, L., & Dondi, L. 1996, A&AS, 120, 503
Ghisellini, G., et al. 2010, MNRAS, 402, 497 (2010)
Ghisellini, G., Ghirlanda, G., Tavecchio, F., Fraternali, F., & Pareschi, G. 2008, MNRAS, 390, L88
Hampf, D., Tluczykont, M., & Horns, D. 2011, arXiv:1104.2336
Hillas, A. M. 1984, ARA&A, 22, 425
Inoue, S. Sigl, G., Miniati, F., & Armengaud, E. 2007, arXiv:astro-ph/0701167
Kang, H., Ryu, D., & Jones, T. W. 1996, ApJ, 456, 422
Kashti, T., & Waxman, E. 2008, JCAP, 05, 006
Kato, T., Kusunose, M., & Takahara, F. 2006, ApJ, 638, 653
Katarzynski, K., Ghisellini, G., Tavecchio, F., Maraschi, L., Fossati, G., Mastichiadis, A. 2005, å, 433, 479
Kneiske, T. M., Bretz, T., Mannheim, K., & Hartmann, D. H. 2004, A&A, 413, 807
Kneiske, T. M., & Dole, H. 2010, A&A, 515, A19
Kotera, K., Allard, D., Murase, K., Aoi, J., Dubois, Y., Pierog, T., & Nagataki, S. 2009, ApJ, 707, 370
Kotera, K., Allard, D., & Lemoine, M. 2011, A&A, 527, A54
Krawczynski, H.; Hughes, S. B.; Horan, D.; Aharonian, F.; Aller, M. F.; Aller, H., et al. 2004, ApJ, 601, 151
Lee, S. 1998, Phys. Rev. D, 58, 043004
Lemoine, M., & Waxman, E. 2009, JCAP, 11, 009
Levinson, A. 2000, Phys. Rev. Lett., 85, 5
Mastichiadis, A., & Kirk, J. G. 1997, A&A, 320, 19

Migliori, G., Grandi, P., Torresi, E., Dermer, C., Finke, J., Celotti, A., Mukherjee, R., Errando, M., Gargano, F., Giordano, and F., Giroletti, M. 2011, arXiv:1107.4302 (accepted to A&A)
Mücke, A., & Protheroe, R. J. 2001, Astropart. Phys., 15, 121
Mücke, A., et al. 2000, Comp. Phys. Comm., 124, 290
Mücke, A., et al. 2003, Astropart. Phys., 18, 593
Murase, K. 2009, Phys. Rev. Lett., 103, 081102
Murase, K., & Beacom, J. F. 2010, Phys. Rev. D, 81, 123001
Murase, K., & Takami, H. 2009, ApJ, 690, L14
Murase, K., Ioka, K., Nagataki, S., & Nakamura, T. 2008a, Phys. Rev. D, 78, 023005
Murase, K., Takahashi, K., Inoue, S., Ichiki, K., & Nagataki, S. 2008b, ApJ, 686, L67
Neronov, A., & Semikoz, D. V. 2007, JETP Lett., 85, 473
Neronov, A., & Vovk, I. 2010, Science, 328, 73
Neronov, A., Semikoz, D., & Vovk, I. 2010, A&A, 519, L6
Neronov, A., Semikoz, D. V., & Taylor, A. M. 2011, arXiv:1104.2801
Norman, C. A., Melrose, D. B., & Achterberg, A. 1995, ApJ454, 60
Ohira, Y., Murase, K., & Yamazaki, R. 2010, A&A, 513, A17
Padovani, P., & Urry, C. M. 1990, ApJ, 356, 75
Pe'er, P., Murase, K., & Mészáros, P. 2009, Phys. Rev. D80, 123018
Perkins, J. S., & VERITAS Collaboration 2010, BAAS, 42, 708
Pian, E., et al. 1998, ApJ, 492, L17
Plaga, R. 1995, Nature, 374, 430
Rachen, J. P., & Biermann, P. L. 1993, A&A, 272, 161
Razzaque, S., Dermer, C. D., and Finke, J. 2011, ApJ, submitted
Rordorf, C., Grasso, D., & Dolag, K. 2004, Astropart. Phys., 22, 167
Ryu, D., et al. 2008, Science, 320, 909
Sandoval, A., et al. 2009, arXiv:0912.3329
Silva, L., Granato, G. L., Bressan, A., & Danese, L. 1998, ApJ, 509, 103
Spiering, C. 2011, Nucl. Inst. Meth. Phys. Res. A, 626, 548
Tagliaferri, G., Ravasio, M., Ghisellini, G., Tavecchio, F., Giommi, P., Massaro, E., Nesci, R., Tosti, G. 2003, A&A, 412, 711
Tagliaferri, G., Foschini, L., Ghisellini, G., Maraschi, L., Tosti, G,; Albert, J., Aliu, E., Anderhub, H. et al. 2008, ApJ, 679, 1029
Takahara, F. 1990, Prog. Theor. Phys., 83, 1071
Takahashi, K., Mori, M., Ichiki, K., & Inoue, S. 2011, arXiv:1103.3835
Takami, H., Yoshiguchi, H., & Sato, K. 2006, ApJ, 639, 803
Takami, H., & Sato, K. 2009, Astropart. Phys., 30, 306
Takami, H., Murase, K., Nagataki, S., & Sato, K. 2009, Astropart. Phys., 31, 201
Takami, H., & Horiuchi, S. 2011, Astropart. Phys., 34, 749
Tavecchio, F,., Maraschi, L., & Ghisellini, G. 1998, ApJ, 509, 608
Tavecchio, F. Ghisellini, G., Ghirlanda, G., Foschini, L., Maraschi, L. 2010, MNRAS, 401, 1570
Tavecchio, F., Ghisellini, G., Bonnoli, G., & Foschini, L. 2011, MNRAS, 570,
Taylor, A. M., Vovk, I., & Neronov, A. 2011, A&A, 529, A144
Tinyakov, P. G., & Tkachev, I. I. 2001, Soviet Journal of Experimental and Theoretical Physics Letters, 74, 445
Urry, C. M., & Padovani, P. 1995, PASP, 107, 803
Vallée, J.P. 2004, New Astron. Rev., 48, 763 (2004)
Vietri, M. 1995, ApJ, 453, 883 (1995).
Wagner, S. J., & HESS collaboration 2010, AAS/High Energy Astrophysics Division #11, 11, #27.06
Wang, X.-Y., Razzaque, S., & Mészáros, P. 2008, ApJ, 677, 432
Waxman, E. 1995, Phys. Rev. Lett. 75, 386
Waxman, E., & Bahcall, J. 1999, Phys. Rev. D, 59, 023002
Zacharopoulou, O., Khangulyan, D., Aharonian, F. A., & Costamante, L. 2011, arXiv:1106.3129